2007 IEEE International Conference on
Robotics and Automation
Roma, Italy, 10-14 April 2007

An Optimum Design of Robotic Hand for Handling a Visco-elastic Object Based on Maxwell Model

Naoki Sakamoto, Mitsuru Higashimori, Toshio Tsuji, and Makoto Kaneko

***Abstract*— This paper discusses an optimum design approach for robotic hands by considering the characteristics of visco-elasticity of food. "Norimaki-sushi" is taken as an example for food. We first show that the dynamic characteristics of such food can be expressed by utilizing the Maxwell model with two layers. Based on dynamic parameters obtained by experiments, we show the relationship among the total working time, the plastic deformation of food after the grasping motion, the hand stiffness, and the operating velocity of the hand. We newly found an interesting behavior of food that allows to find an optimum set of the design parameters for achieving the minimum plastic deformation of food.**

I. INTRODUCTION

At present, dishing up food into a box lunch sold at convenience stores is done manually by workers standing on both sides of a belt conveyor, as shown in Fig.1. The net profit of an individual box lunch, that is, the sales price minus the cost of the raw food materials, personnel expenses and other management costs, is limited to roughly 2% of the retail store price. To increase net profit or to improve the profit ratio for dealing in box lunches, the manual processes for dishing up should be shifted to an automatic sorting and filling system. When designing a robotic hand for handling food, compared to a robotic hand for industrial applications, the visco-elasticity, adhesiveness, and non-homogeneity of objects have to be considered. In this work, we focus on the visco-elasticity of the handled objects and pick up the vinegared rice rolled in laver, so called Norimaki-sushi(or Norimaki). The visco-elastic characteristics of food have been established by using an approximate model based on the Maxwell Model using two different elements, i.e., the elastic element and the viscous element [1], as shown in Fig.2(a). Handling such a visco-elastic object by a robotic hand can be classified into three phases; the closing phase where the hand base position closes for increasing the grasping force applied to the object, as shown in Fig.2(i), the stationary phase where the hand base position is fixed and the grasping force decreases by the plastic deformation of the object, as shown in Fig.2(ii), and the opening phase where the hand base position opens for releasing the object, as shown in Fig.2(iii). Through all phases, the grasping force f changes with respect to time. The grasping force also changes with the stiffness of the hand. In order to design a robotic hand for use in dishing up food for box lunches, there are a couple of requirements, including a) lying a total working time cycle T of the robot system within a remunerative time period, b) holding up the object for a prescribed time period T_l for transporting the object, and c) restraining the plastic deformation of object X_p within an acceptable range to ensure product quality. Taking the above requirements and the characteristics of object into account, this paper explores

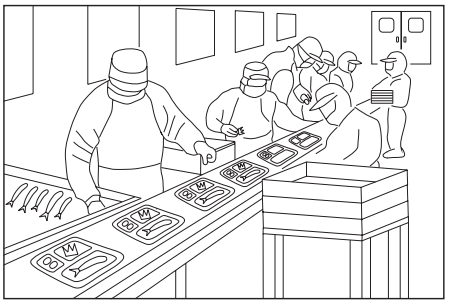

Fig. 1. Production factory of box lunches.

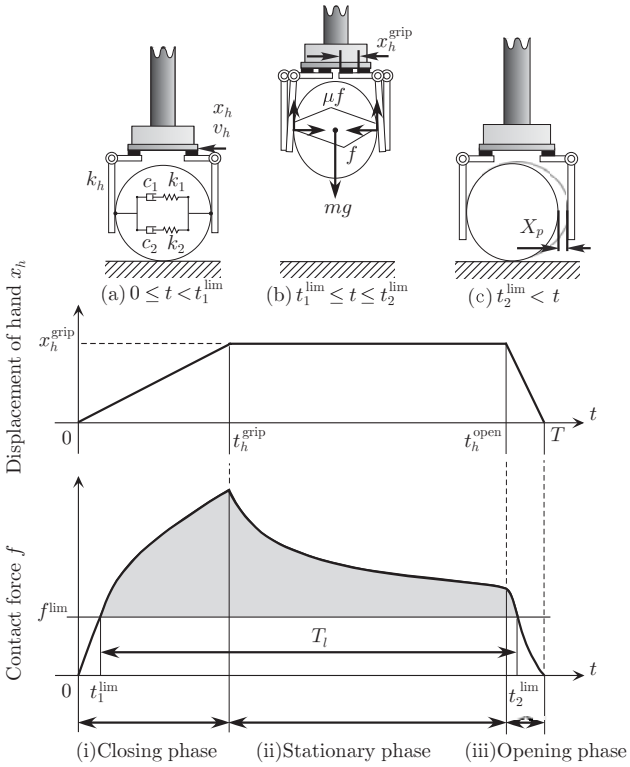

Fig. 2. Three phases for handling a food.

N. Sakamoto is with Mayekawa Mfg. Co., Ltd., 2000 Tatsusawa, Moriya, Ibaraki, 302-0118, Japan naoki-sakamoto@mayekawa.co.jp

M. Higashimori and M. Kaneko are with Department of Mechanical Engineering, Osaka Univ., 2-1 Yamadaoka, Suita, Osaka, 565-0871, Japan {higashi, mk}@mech.eng.osaka-u.ac.jp

T. Tsuji is with Department of Artificial Complex Systems Engineering, Hiroshima Univ., 1-4-1 Kagamiyama, Higashihiroshima, Hiroshima, 739-8527, Japan tsuji@bsys.hiroshima-u.ac.jp

how the plastic deformation X_p and the total working time T change with respect to the design parameters (the hand stiffness and the operating velocity of the hand).

This paper discusses a design approach for robotic hands by considering the characteristics of visco-elasticity and hopefully finds an optimum set of design parameters. This paper is organized as follows; In chapter II, we briefly review related works. In chapter III, we obtain the visco-elastic parameters of Norimaki through experiments and show that such a characteristic can be approximated by a Maxwell model. In chapter IV, we explore the relationship among the hand stiffness, the operation velocity of the hand, the resultant plastic deformation of the object after being released, and the total working time. Based on this relationship, we show an interesting observation where there exists the minimum plastic deformation of object with respect to the operating velocity of the hand exists. In chapter V, we solve an optimum design problem for the hand. We obtain the optimum combination of the hand stiffness and the operating velocity so that either the plastic deformation or the total working time results in minimum. In chapter VI, we give the conclusion of this work.

II. Related Works

Robotic systems and automations for food processing have been desired by the food industry for a long time. As for deformations of food, Tokumoto and et al. [2] have shown that a proper combination of both elastic and viscous elements can express the basic behavior of rheology objects. They have also shown simulation results for confirming the validity of the model. As for food handling robots, Li and Lee [3] have developed a visually guided robotic system for handling food. They have shown that the gripper grasps robustly non-homogeneity food by visual information. Silsoe Research Institute [4] have developed the creative robot hand so that handling for a food which has adhesion. The hand is composed by a pair of gripping finger and film such as belt conveyor, can release the adhesion object accurately. Tomizawa et al. [5] have proposed a multi-fingered hand with an acetabulum at the top of each finger, for handling fresh fruits. They have shown that the proposed hand has the potential to grasp an object by using the acetabulums without damaging the object. Mayekawa Mfg. Co., Ltd. [6] has developed a poultry thigh leg deboning robot which can work approximately four times faster than a human and process approximately 900 poultry thigh parts per hour. Also, as for handling soft objects other than food, Taylor et al. [7] have discussed the automatic handling for shoes and garment. Hirai et al. [8] have discussed the strategy for handling thin deformable objects such as sheets metal or leather products. Wada et al. [9] have proposed the control method for textile fabrics, where the position, posture, and deformation of an object can be controlled by utilizing a vision sensor to detect the position of representative predetermined points on the object. Zheng et al. [10] have discussed how to set up a flexible beam with mounting holes in order to automatic assembly tasks.

III. Dynamic Characteristic of Food

A. General Concept

In general, it is well known that food has rheological characteristics which can be well approximated by a dynamic model using elastic and viscous elements [1]. In this work, suppose a small deformation of food, we approximate the non-linear characteristics of food by a four-element Maxwell model, as shown in Fig.2(a), which has connection of two parallel units where each unit is a serial elastic element and a viscous element. In Fig.2(a), k_i and c_i are the elastic and the viscous coefficient of the i-th layer ($i = 1, 2$), respectively. Now, let us consider that an external force f acts on the object. When denoting by x, x_i, and f_i the whole deformation of the object, the deformation of the i-th layer, and the force applied to the i-th layer, respectively, we can obtain the following relationship:

$$f_i(t) = k_i x_{ki} = c_i \dot{x}_{ci}, \tag{1}$$

$$f(t) = \sum f_i(t), \tag{2}$$

$$x = x_i = x_{ki} + x_{ci}, \tag{3}$$

where x_{ki} and x_{ci} are the deformation of the elastic and the viscous element, respectively, of the i-th layer. By removing f_i, x_i, x_{ki}, and x_{ci} from (1)–(3), we can derive the following equation:

$$b_2 \ddot{x}(t) + b_1 \dot{x}(t) = a_2 \ddot{f}(t) + a_1 \dot{f}(t) + f(t), \tag{4}$$

where

$$b_2 \triangleq \frac{c_1 c_2 (k_1 + k_2)}{k_1 k_2}, \tag{5}$$

$$b_1 \triangleq c_1 + c_2, \tag{6}$$

$$a_2 \triangleq \frac{c_1 c_2}{k_1 k_2}, \tag{7}$$

$$a_1 \triangleq \frac{c_1 k_2 + c_2 k_1}{k_1 k_2}. \tag{8}$$

Equation(4) is the differential equation expressing the relationship between the external force applied to the object f and the deformation x of the object.

B. How to Estimate Parameters of Norimaki

Suppose that an object with visco-elastic parameters c_i and k_i is grasped by a hand with stiffness k_h, as shown in Fig.2. By letting x_h be the displacement of the base of hand, we obtain

$$x(t) = x_h(t) - \frac{f(t)}{k_h}. \tag{9}$$

From (4) and (9), we can obtain

$$B_2 \ddot{x}_h(t) + B_1 \dot{x}_h(t) = A_2 \ddot{f}(t) + A_1 \dot{f}(t) + f(t), \tag{10}$$

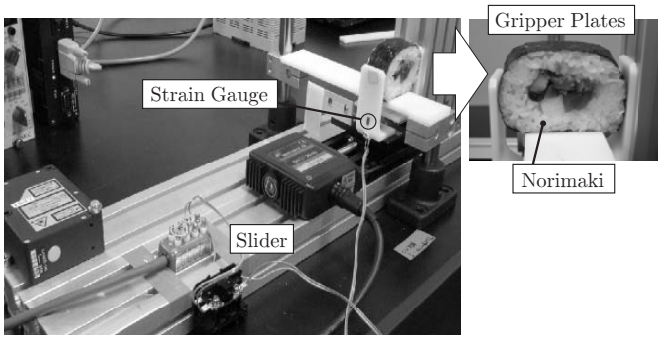

Fig. 3. An overview of the experimental system.

where

$$B_2 \triangleq \frac{c_1 c_2 (k_1 + k_2)}{k_1 k_2}, \quad (11)$$

$$B_1 \triangleq c_1 + c_2, \quad (12)$$

$$A_2 \triangleq \frac{c_1 c_2 (k_h + k_1 + k_2)}{k_h k_1 k_2}, \quad (13)$$

$$A_1 \triangleq \frac{c_1 k_2 (k_h + k_1) + c_2 k_1 (k_h + k_2)}{k_h k_1 k_2}. \quad (14)$$

Based on (10), we experimentally obtain the visco-elastic parameters c_i and k_i of Norimaki. Now, suppose that the hand makes contact with the object. The contact force is zero at the initial phase ($t = 0$, $x_h = 0$). We give open and close commands to the hand by the following procedure:

1. Closing phase ($0 \leq t < t_h^{\text{grip}}$) : Close the hand for the position of $x_h = x_h^{\text{grip}}$ with the operating velocity of $v_h (= \dot{x}_h)$, as shown in Fig.2(i).
2. Stationary phase ($t_h^{\text{grip}} \leq t < t_h^{\text{open}}$) : Fix the hand at $x_h = x_h^{\text{grip}}$, as shown in Fig.2(ii).
3. Opening phase ($t_h^{\text{open}} \leq t \leq T$) : Open the hand to the position of $x_h = 0$ with the operating velocity of v_h, as shown in Fig.2(iii).

Fig.3 gives an overview of the experimental system, where a dummy hand with two parallel grippers with the stiffness of k_h is utilized. One gripper is fixed on the base and the other can be moved by a linear slider, so that they can realize smooth opening and closing motions. The base displacement of the gripper $x_h(t)$ is measured by an encoder integrated in the motor for driving the slider. The normal component of contact force at the contact point $f(t)$ is measured by the strain gauge attached to the gripper. By inserting the measured $x_h(t)$ and $f(t)$ into (10), we can compute A_1, A_2, B_1, and B_2. Instead of using the differential (10), which introduces a large error by differentiating the noisy signal, we transform (10) to the following integration equation:

$$\boldsymbol{M}\boldsymbol{p} = \boldsymbol{q}, \quad (15)$$

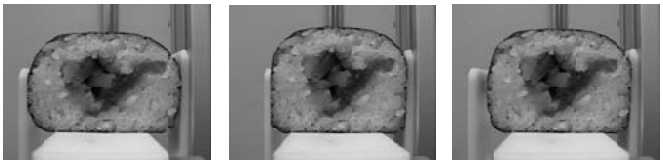

(a) $t = 0$[s] (b) $t = 3$[s] (c) $t = 6$[s]

Fig. 4. A series of photo during a whole experiment.

where

$$\boldsymbol{M} \triangleq \left[-\boldsymbol{f}, \ -\int \boldsymbol{f} dt, \ \boldsymbol{x}_h, \ \int \boldsymbol{x}_h dt \right], \quad (16)$$

$$\boldsymbol{p} \triangleq [A_2, A_1, B_2, B_1]^T, \quad (17)$$

$$\boldsymbol{q} \triangleq \iint \boldsymbol{f} dt^2, \quad (18)$$

$$\boldsymbol{f} \triangleq [f(t_1), f(t_2), \ldots, f(t_n)]^T, \quad (19)$$

$$\boldsymbol{x}_h \triangleq [x_h(t_1), x_h(t_2), \ldots, x_h(t_n)]^T, \quad (20)$$

$f(t_i)$ and $x_h(t_i)$ are the contact force and the base displacement of hand, respectively, at the sampling time t_i ($i = 1, 2, \cdots, n$). From (15), we can estimate $\boldsymbol{p}$ by the least squares method as follows:

$$\boldsymbol{p} = (\boldsymbol{M}^T \boldsymbol{M})^{-1} \boldsymbol{M}^T \boldsymbol{q}. \quad (21)$$

After computing $\boldsymbol{p}$ by using experimental data, the visco-elastic parameters c_i and k_i can be computed from (11)–(14), as follows:

$$k_1 = \frac{-2A_2B_1 + (A_1 + \sqrt{A_1^2 - 4A_2})B_2}{2A_2\sqrt{A_1^2 - 4A_2}}, \quad (22)$$

$$k_2 = \frac{2A_2B_1 - (A_1 - \sqrt{A_1^2 - 4A_2})B_2}{2A_2\sqrt{A_1^2 - 4A_2}}, \quad (23)$$

$$c_1 = \frac{2B_2 - (A_1 - \sqrt{A_1^2 - 4A_2})B_1}{2\sqrt{A_1^2 - 4A_2}}, \quad (24)$$

$$c_2 = \frac{-2B_2 + (A_1 + \sqrt{A_1^2 - 4A_2})B_1}{2\sqrt{A_1^2 - 4A_2}}. \quad (25)$$

C. Results of Estimation

We adopt a popular Norimaki as an object for the experiment. Fig.4 show a series of photos taken during an experiment, where the hand stiffness is $k_h = 8500$[N/m], the operating velocity is $v_h = 20$[mm/s], the base displacement is $x_h^{\text{grip}} = 8$[mm], the time for finishing the closing motion is $t_h^{\text{grip}} = 0.8$[s], and the time for starting the opening motion is $t_h^{\text{open}} = 5.0$[s], respectively. Fig.4(a), (b), and (c) show the object and the hand at times $t = 0$[s], $t = 3$[s], and $t = 6$[s], respectively. The continuous line in Fig.5 shows the contact force between the hand and the object with respect to time. From this line, we can see that: the contact force increases in the closing phase ($0 \leq t < 0.8$[s]), the contact force relaxes as time passes in the stationary phase ($0.8 \leq t < 5.0$[s]), and the contact force rapidly decreases in the opening phase ($5.0 \leq t \leq 5.5$[s]). The visco-elastic parameters c_i and k_i,

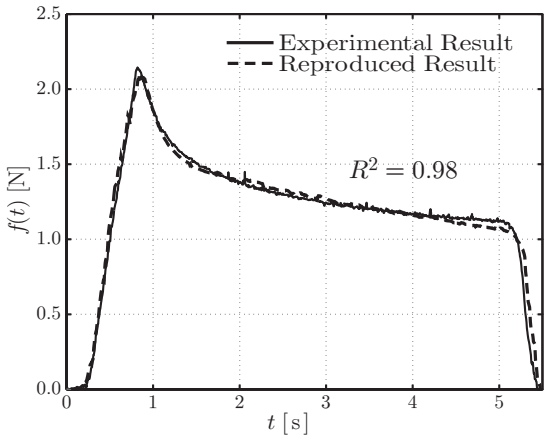

$k_1 = 220[\mathrm{N/m}] \quad k_2 = 130[\mathrm{N/m}]$
$c_1 = 35[\mathrm{Ns/m}] \quad c_2 = 1400[\mathrm{Ns/m}]$

Fig. 5. The output of $f(t)$ with respect to time.

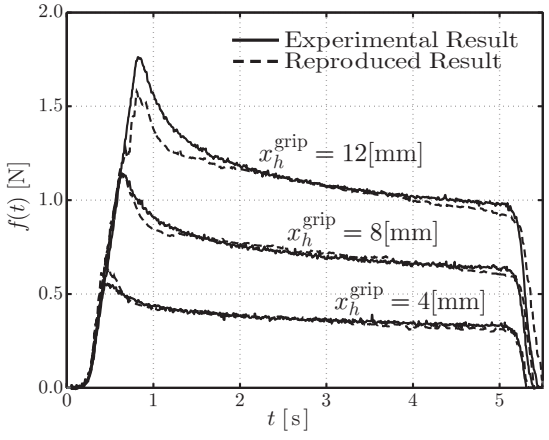

$k_1 = 200[\mathrm{N/m}] \quad k_2 = 110[\mathrm{N/m}]$
$c_1 = 20[\mathrm{Ns/m}] \quad c_2 = 1400[\mathrm{Ns/m}]$

Fig. 6. The output of $f(t)$ with respect to time under various x_h^{grip}.

which are estimated by using the contact force data in Fig.5, are indicated in Fig.5. The dashed line in Fig.5 shows the reproduced contact force computed by using (10)-(14) with the estimated parameters k_i, c_i and the hand position data $x_h(t)$. We can see that the reproduced contact force nicely matches with the contact force obtained by the experiment, where the degree of approximation is given by $R^2 = 0.98$. In order to obtain the average parameters of Norimaki, we execute 10 experiments for each of the three base displacements $x_h^{\mathrm{grip}} = \{4, 8, 12\}$[mm], and performed 30 the estimations. In Fig.6, we show the average of estimated visco-elastic parameters. The continues line and the dashed line in Fig.6 show one of the experimental contact force and the reproduced contact force, respectively, for $x_h^{\mathrm{grip}} = \{4, 8, 12\}$ [mm]. The average of parameters in Fig.6 are utilized for analysis in Chapter IV and thereafter.

IV. Preparation toward Designing Hand

In this chapter, we explore the relationship between the design parameters of the hand and the food characteristic as shown in Fig.2, where we regard the hand stiffness k_h and the operating velocity v_h as the design parameters of the hand.

A. Definition of Plastic Deformation and Total Working Time

For a given set of the base displacement of the hand in the stationary phase x_h^{grip} and the operating velocity in the closing phase v_h, the time for finishing the closing phase t_h^{grip} is determined as follows:

$$t_h^{\mathrm{grip}} = \left| \frac{x_h^{\mathrm{grip}}}{v_h} \right|. \tag{26}$$

On the other hand, the time for starting the opening phase t_h^{open} has to be determined according to the transporting time T_l. Suppose that the transporting time T_l is given. For avoiding that the hand drops the object, the following condition for the normal component of the contact force is required:

$$mg\alpha \leq 2\mu f, \tag{27}$$

where m, g, μ, and α are the mass of object, the gravitational acceleration, the friction coefficient between the hand and the object, and the safety factor[1], respectively. From (27), we can express the limitation of contact force as follows:

$$f^{\mathrm{lim}} \triangleq \frac{mg\alpha}{2\mu}. \tag{28}$$

Suppose that in the closing phase and the opening phase, there are unique times at which $f(t) = f^{\mathrm{lim}}$, as shown in Fig.2. Such times t_1^{lim} and t_2^{lim} are defined by the following conditions:

$$t_1^{\mathrm{lim}} \triangleq t|_{f=f^{\mathrm{lim}}} \quad (0 \leq t_1^{\mathrm{lim}} \leq t_h^{\mathrm{grip}}), \tag{29}$$
$$t_2^{\mathrm{lim}} \triangleq t|_{f=f^{\mathrm{lim}}} \quad (t_h^{\mathrm{open}} \leq t_2^{\mathrm{lim}} \leq T). \tag{30}$$

To guarantee that the hand can support the object for the time T_l of the transport of object, the following condition is further required:

$$t_2^{\mathrm{lim}} - t_1^{\mathrm{lim}} \geq T_l. \tag{31}$$

To minimize the total working time T, let us consider the time for starting the opening phase t_h^{open} so that it leads to

$$t_2^{\mathrm{lim}} - t_1^{\mathrm{lim}} = T_l. \tag{32}$$

Under the above t_h^{grip} and t_h^{open}, we define the total working time T and the plastic deformation X_p as follows:

$$T \triangleq t_h^{\mathrm{open}} + \left| \frac{x_h^{\mathrm{grip}}}{v_h^{\max}} \right|, \tag{33}$$
$$X_p \triangleq x(\infty). \tag{34}$$

[1] $\alpha \geq 1$ indicates how much larger the friction force is required to be than the gravity force applied to the object. However, an excessively large α leads to a large contact force, and as a result, to a large plastic deformation.

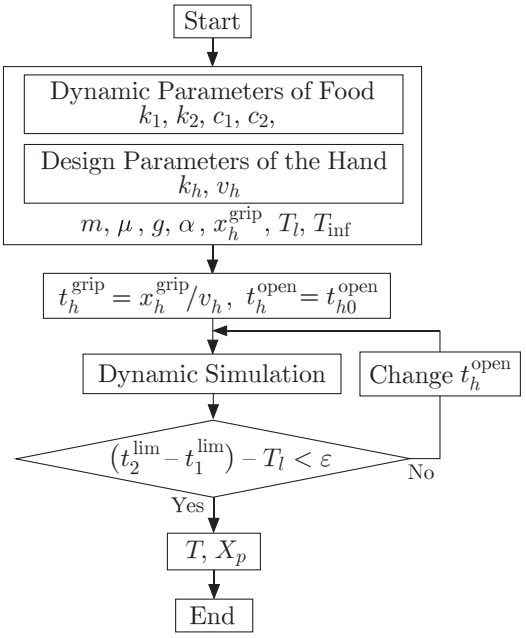

Fig. 7. Flowchart for obtaining T and X_p.

TABLE I

PARAMETERS FOR SIMULATION.

k_1	stiffness of the 1st spring	200 [N/m]
k_2	stiffness of the 2nd spring	110 [N/m]
c_1	viscosity of the 1st damping	20 [Ns/m]
c_2	viscosity of the 2nd damping	1400 [Ns/m]
T_l	time for lifting object	2.0 [s]
m	mass of object	0.045 [kg]
μ	coefficient of friction	1.2
g	acceleration due to gravity	9.8 [m/s^2]
$x_h^{\rm grip}$	base displacement of hand	8.0 [mm]
$v_h^{\rm min}$	minimum speed of the hand	2.0 [mm/s]
$v_h^{\rm max}$	maximum speed of the hand	200 [mm/s]
$k_h^{\rm min}$	minimum stiffness of hand	500 [N/m]
$k_h^{\rm max}$	maximum stiffness of hand	100000 [N/m]
α	safety factor	3
$T_{\rm inf}$	additional time for recovery of food	3.0 [s]

where the hand opens with the maximum velocity $v_h^{\rm max}$ in the opening phase, for simplicity, we like to note that the plastic deformation is caused by the deformation of viscous elements.

B. Relationship among Design Parameters, Plastic Deformation, and Total Working Time

In this section, we discuss the relationship among the hand stiffness k_h, the operating velocity of the hand v_h, the total working time T, and the plastic deformation X_p. For the hand motion in each phase, the behavior of the object can be computed by simulation based on (10). Fig.7 shows the flowchart for obtaining T and X_p. Instead of using (34), the plastic deformation is computed by $X_p = x(T + T_{\rm inf})$, where $T_{\rm inf}$ is given large enough for the object to finish the recovering motion after being released. Table I shows the parameters used for the simulation. Fig.8 shows the total working time T and the plastic deformation X_p under the variable parameters of the hand stiffness $k_h^{\rm min} \le k_h \le k_h^{\rm max}$ and the operating velocity $v_h^{\rm min} \le v_h \le v_h^{\rm max}$. In addition, Fig.9–Fig.11 show the relationships between two parameters in Fig.8.

Fig.9 shows the relationship between the hand stiffness k_h and the plastic deformation X_p. From this figure, we can see that the plastic deformation X_p monotonously increases as the hand stiffness k_h becomes larger, except for the case where the operating velocity v_h is extremely small. When the hand stiffness k_h is large, the contact force applied to the object becomes large, and as a result, the deformation of viscous elements becomes large.

Fig.10 shows the relationship between the hand stiffness k_h and the total working time T. From this figure, we can see that the total working time T monotonously decreases as the hand stiffness k_h becomes larger. As the hand stiffness

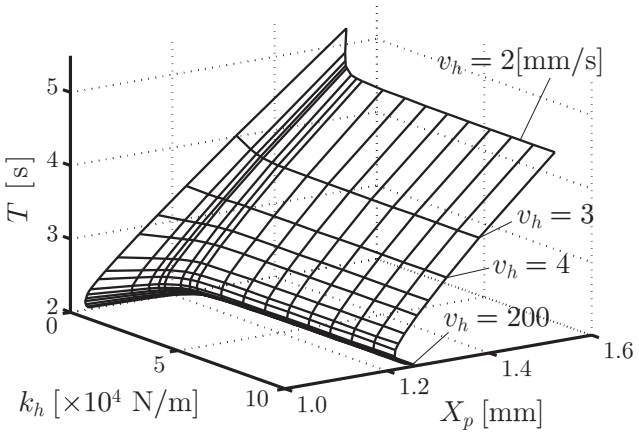

Fig. 8. The relationship among v_h, k_h, X_p, and T.

k_h becomes larger, the force required to hold up the object $f^{\rm lim}$ is generated earlier, and as a result, the total working time T becomes smaller.

Fig.11 shows the relationship between the operating velocity v_h and the plastic deformation X_p. From this figure, we can see that the plastic deformation X_p becomes large in the case where the operating velocity v_h is extremely small, while it is sharply decreases as the operating velocity v_h becomes larger. Let us now consider the reason by using the 1-layer Maxwell model for simplicity. Fig.12(a) shows the displacements of elastic and viscous elements under the operating velocity $v_h \approx 0$, where (i) and (ii) correspond to the time when the closing phase finishes ($t = t_h^{\rm grip}$) and the time when the opening phase starts ($t = t_h^{\rm open}$), respectively. As shown in Fig.12(a-i), the work done by the hand in the closing phase is entirely assigned to the

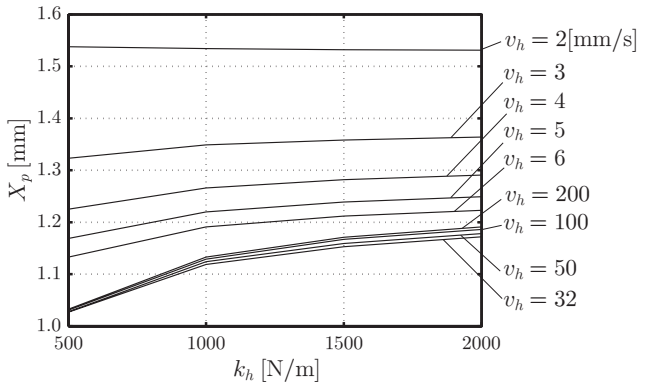

Fig. 9. The relationship between k_h and X_p.

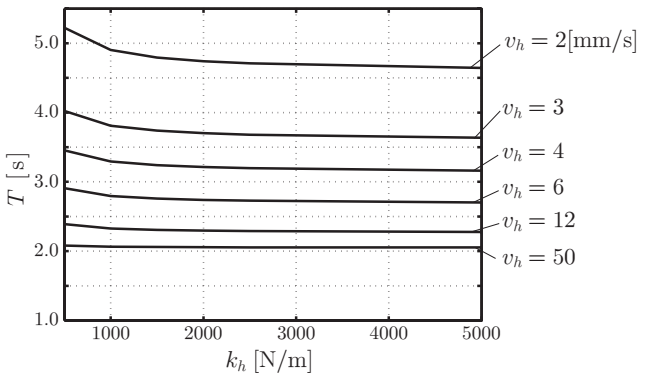

Fig. 10. The relationship between k_h and T.

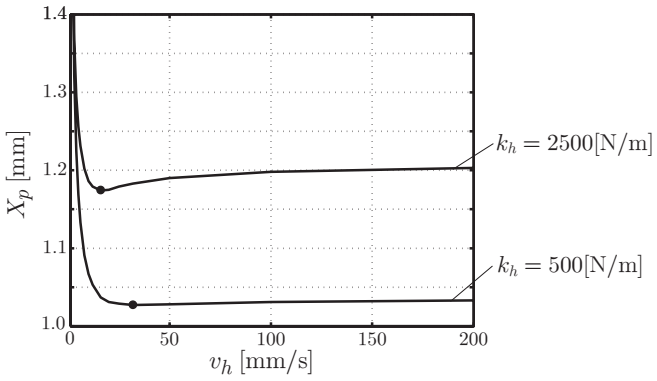

Fig. 11. The relationship between v_h and X_p.

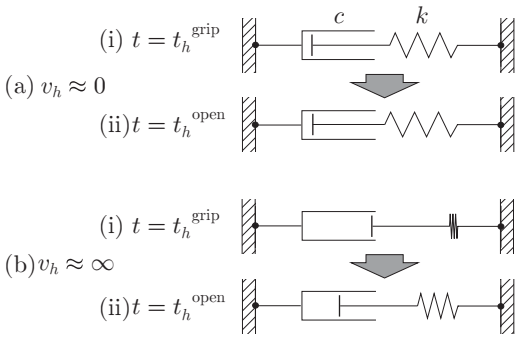

Fig. 12. Displacements by both elastic and viscous elements during the stationary phase of hand.

displacement of the viscous element, in the case where the operating velocity v_h is extremely small. Then, as shown in Fig.12(a-ii), no recovery of the viscous element is generated in the stationary phase. Since no recovery occurs in the opening phase, the large displacement of the viscous element finally remains. On the other hand, under the operating velocity $v_h \approx \infty$, as shown in Fig.12(b-i), the work done by the hand in the closing phase is entirely accumulated into the elastic energy and no displacement of the viscous element is generated in the closing phase. As shown in Fig.12(b-ii), a portion of the accumulated energy is then used for the displacement of the viscous element, in the stationary phase. In the opening phase, however, the rest of the accumulated energy is released. This is the reason why the increase of the operating velocity v_h is effective for suppressing the plastic deformation X_p.

Now, we would note that there is a remarkable observation where the plastic deformation X_p results in minimum, as shown by • in Fig.11, with respect to the operation velocity v_h. This is supposed to be caused by the exquisite balance between the operating velocity and the grasping time in the stationary phase. As far as we know, such an interesting observation has not been reported in the past. This property may become important for designing robots for handling the food which especially requires a large attention on the deformation.

V. Examples of Optimum Design

Let us now replace the discussion in Chapter IV by the optimum design problem to minimize either the plastic deformation X_p or the total working time T. We formulate these optimum problems as follows:

$$
\begin{array}{ll}
\text{Minimize} & X_p \text{ (or } T) \\
\text{Subject to} & f^{\lim} \le f(t), \;\; t_1^{\lim} \le t \le t_2^{\lim}, \\
& t_2^{\lim} - t_1^{\lim} \ge T_l, \\
& T \le T^{\max} \text{ (or } X_p \le X_p^{\max}), \\
& v_h^{\min} \le v_h \le v_h^{\max}, \\
& k_h^{\min} \le k_h \le k_h^{\max},
\end{array}
$$

where $T^{\max}$ and $X_p^{\max}$ are the permissible total working time and the permissible plastic deformation, respectively, and the decision variables are the operation velocity v_h and the hand stiffness k_h, respectively.

Minimum Plastic Deformation: Fig.13 is obtained by enlargement of the simulation results shown in Fig.8 within the range of $0 < k_h \le 5000$ [N/m] and $10 \le v_h \le 200$ [mm/s], respectively. When $T^{\max} = 2.20$[s] is given, for example, the minimum plastic deformation X_p obtained from Fig.13 is $Xp = 1.03$[mm] (Point A indicated in Fig.13). In this case, the optimum operating velocity v_h^*, the optimum stiffness k_h^*, and the minimum plastic deformation X_p are also obtained and given by $v_h^* = 32$[mm/s], $k_h^* = 500$[N/m], and $T = 2.12$[s], respectively.

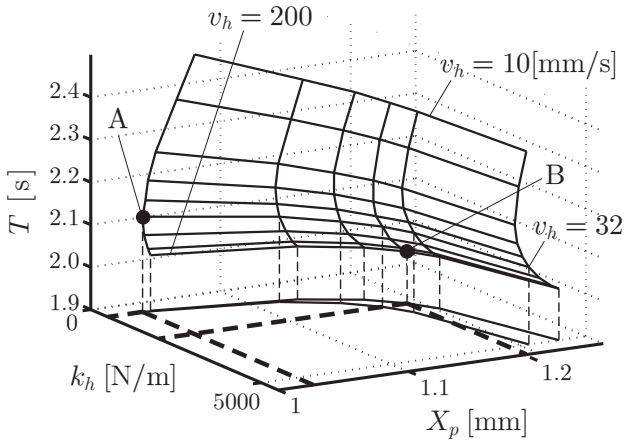

Fig. 13. The optimum design point.

(a) $t = 0$[s] (b) $t = 0.7$[s] (c) $t = 2.1$[s]

Fig. 14. An overview of demonstration.

Minimum Total Operating Time: When $X_p^{\max} = 1.2$[mm] is given, the minimum total working time T can be obtained from Fig.13, i.e., $T = 2.02$[s] (Point B indicated in Fig.13). In this case, v_h^*, k_h^*, and X_p can be also obtained and given by $v_h^* = 200$[mm/s], $k_h^* = 2000$[N/m], and $X_p = 1.2$[mm], respectively.

VI. Conclusion

We discussed an optimum design approach on robot hand for handling food by considering the characteristics of visco-elasticity. The main results are summarized as follows:

1) Based on the four-element Maxwell model, we experimentally obtained the visco-elastic parameters of Norimaki.
2) We showed the relationship among the design parameters of the hand (the stiffness and the operating velocity), the plastic deformation, and the total working time. During simulation, we obtained an interesting observation where the plastic deformation resulted in minimum with respect to the operating velocity.
3) We showed two examples of the optimum design, where we determined the optimum combination of the hand stiffness and the operating velocity of the hand to minimize either the plastic deformation or the total working time.

Finally, Fig.14 shows an demonstration of handling "Norimaki-sushi". In the future, we would like to take into account the adhesion of the object as well as its visco-elasticity for the design of food handling robot hands.

Acknowledgement

The authors thank Mr. Masahiro Yuya at Mitsubishi Electric Corporation. He contributed in every stage of the research.

References

[1] N. N. Mohsenin, "Physical properties of plant and animal materials," *New York Gordon and Breach*, 1970.
[2] S. Tokumoto, S. Hirai, and H. Tanaka, "Constructing Virtual Rheological Objects," *Proc. World Multiconference on Systemics, Cybernetics and Infomatics*, pp.106–111, 2001.
[3] Y. F. Li, M. H. Lee, "Applying Vision Guidance in Robotic Food Handling," *IEEE Robotics & Automation Magazine*, pp.4–12, 1996.
[4] "Gripping Apparatus with Two Fingers Covered by a Moveable Film," International Patent Application WO03011536
[5] T. Tomizawa, A. Ohya, S. Yuta, and E. Koyanagi, "Remote Shopping Robot System for Fresh Foods," *JSME, Conference on Robotics and Mechatronics '05*, 1A1-N-027, 2005 (in Japanese).
[6] R. Kodama, N. Machida, and I. Ito, "Automatic measurement for the knee joint cutting position of Poultry Leg Meat by RT," *SICE System Integration Division Annual Conference(SI2003)*, pp.806–807, 2003 (in Japanese).
[7] P.M. Taylor, et al, "Sensory Robotics for the Handling of Limp Materials," *Springer-Verlag*, 1990.
[8] S. Hirai, H. Wakamatsu, and K. Iwata, "Modeling of Deformable Thin Parts for Their Manipulation," *Proc. of IEEE Int. Conf. on Robotics and Automation*, pp.2955–2960, 1994.
[9] T. Wada, S. Hirai, H. Mori, and S. Kawamura, "Robust Manipulation of Deformable Objects Using Model Based Technique," *H. H. Nagel and F. J. Perales eds, First Int. Workshop on Articulated Motion and Deformable Objects(AMDO 2000), Lecture Note in Computer Science*, no.1899, pp.1–14, Springr-Verlag, 2000.
[10] Y. F. Zheng, R. Pei, and C. Chen, "Strategies for Automatic Assembly of Deformable Objects," *Proc. of IEEE Int. Conf. on Robotics and Automation*, pp.2598–2603, 1991.